MICROWAVE NOISE FIELD BEHAVES LIKE WHITE LIGHT

J. Polivka

Spacek Labs. Inc.
212 E. Gutierrez St., Santa Barbara, CA 93101, U.S.A.

P. Fiala

Brno University of Technology
Czech Republic

J. Machac

Czech Technical University in Prague
Czech Republic

Abstract—This paper presents various applications where wide-band signals are the dominant factor. The approaches applied here are based on the present knowledge in the field of white light theory (the THz band), the particle theory of light, and the wave theory of light. White light theory is used to investigate wide-band applications of non-coherent electromagnetic waves in the GHz range represented by noise. In addition, the theoretical approaches to the field of white light are confirmed by various experiments with noise fields applied in the GHz range. These experiments show clear advantages of measurements performed by means of noise fields. The most important feature of these fields is the absence of interference effects.

1. INTRODUCTION

In classical optics, no full description theory of "white light" has yet been conceived. In his "Opticks", Newton proposed a corpuscular hypothesis, but Young's experiment proved the wave basis of light. De Broglie united these two concepts as the "wave-particle" concept [1]. The wave concept has been used for microwaves, as the photon energy

was found to be too weak. The wideband spectrum solution of luminous relations (luminous flux, luminosity) applying transformation function V_λ [2] to the sensitivity of the human eye is not directly applicable to a description of wideband and ultra-wideband (UWB) electromagnetic waves; it is, however, a useful direction in describing the theoretical solution of microwave noise. The modified lighting theory is presented here with some special features of microwave random field behavior.

There are various approaches to the area of wideband spectrum electromagnetic wave propagation. The first approach, well known from lighting technology as the ray technique, accepts the propagation directions of the wideband spectrum signal and solves the reflection and absorption on the boundaries. The changes of complex angles of accidence and reflection, as well as changes of wave polarization, are solved using only a nonlinear correcting curve related to a reference sensor — the human eye. In this way, a description is acquired not of the phase changes and wave polarization, but only of the amplitudes of an electromagnetic wave. Another approach is based on the solution of partial differential equations (PDE) to describe the proper physical model of electromagnetic wave propagation.

Even before UWB communication and sensing was introduced, the development of low-noise receivers for radar and sensing stimulated the use of the wideband noise concept and radiometry, mainly in the microwave region. Some radiometric principles were utilized to characterize wideband antennas, most often in satellite and space communication.

In an experiment performed by one of the authors, the microwave noise field has been shown to behave like white incoherent light, featuring the properties best described by lighting. In many of his experiments with microwave noise fields, Polivka has observed that these fields are non-coherent, wideband, and present no interference even in the near zone of antennas and radiators [4]. Consequently, he "discovered" the microwave noise fields when he was designing calibration devices and circuits for the microwave radiometers that he developed for atmospheric sensing. The most surprising feature was the absence of interference effects near the radiators. Optical methods like Lloyd's mirror were used to prove that there is no interference around the reflecting surfaces, and other optical approaches were used to describe the noise fields. The as yet not fully elaborated theory of these random fields led to the curious observation that, in the development of classical optics, no "white-light" approach had ever been tried; non-coherent fields were avoided in theoretical books as "no mathematics existed" to describe them.

Polivka's experiments in "active radiometry" were based on the use of two elements: a "noise radiator" and a "radiometer with an antenna", as shown in Fig. 1. Many modifications of the "noise radiators" were made and tested [4]. It was shown that while all the tested noise radiators generated a random field without any local interference, they behaved approximately as Lambertian light sources, which are typical for the diffusion reflection of electromagnetic waves, with spatial intensity distribution like in Fig. 2. This distribution corresponds to the intensity distribution of a dipole antenna.
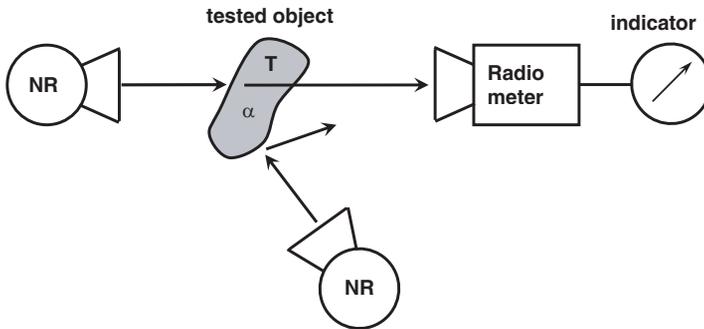
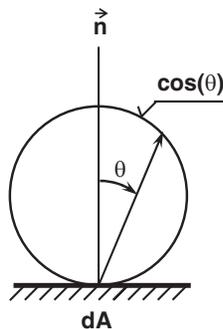**Figure 1.** Noise radiator and radiometer setup in active radiometry.

Figure 2. Field distribution of an optical Lambertian source.

This paper introduces both the basic theoretical formulas of the wideband spectrum model of electromagnetic wave propagation and experimental solutions of effects related to this wave propagation. The paper briefly introduces an evaluation of the suitability of particular quantities from the point of view of ray optics, and the relation of these quantities to the experimental approach of UWB electromagnetic theory.

2. A BASIC DESCRIPTION OF LIGHT ACTIVE ELEMENTS USED IN OPTICS

Radiant energy dQ passing through area A per time dt is known as the radiant flux through this area and represents the power of radiation containing all wavelengths, for a more detailed description, see [6]. So the radiant flux [W] is defined as

$$W_e = \frac{dQ}{dt}. \tag{1}$$

The spectral distribution of the radiant flux in dependence on wavelength is known as the spectral flux density, defined by the differential fraction of radiant flux and wavelength λ

$$\Phi_{e\lambda} = \frac{dW_e}{d\lambda}, \quad W_e = \int\limits_0^\infty \Phi_{e\lambda} d\lambda. \tag{2}$$

The energy of light is the radiant energy related to the defined band of electromagnetic radiation. Most light detectors, including the human eye, are differently sensitive to electromagnetic waves of various wavelengths. Consequently, only a part of the radiant flux depending on the spectral distribution of the electromagnetic wave could be detected. The sensitivity of the human eye, known as the V_λ function, is shown in Fig. 3 [6]. The radiant flux characterizing the power of radiation from a narrow detected spectrum of the visible
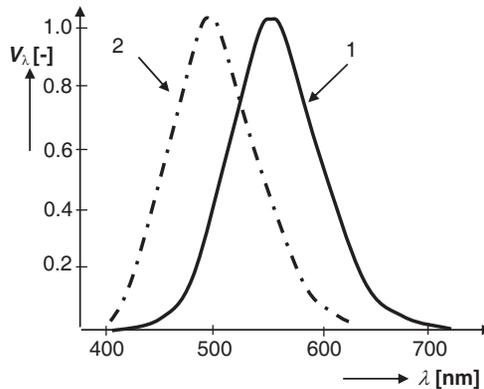

Figure 3. Relative spectral sensitivity of a standard observer. Curve 1 corresponds to photo-optic visual perception (day light), curve 2 represents scoto-optic visual perception (night light) [24].
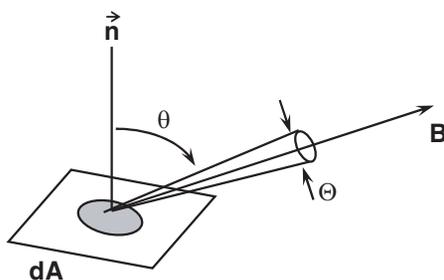
Figure 4. To the definition of luminosity illumination, and radiance.

range is known as the luminous flux [W]

$$W = \int_0^\infty V_\lambda dW_e = \int_0^\infty V_\lambda \Phi_{e\lambda} d\lambda. \tag{3}$$

Luminosity I can be defined only for a point source, namely, for a source whose dimensions are negligible in comparison with the distance between the observer and the source. The luminosity of the point source in the direction determined by angle θ is equal to the luminous flux bound in the solid angle Θ, see Fig. 4, and is defined by

$$I = \frac{dW}{d\Theta} \tag{4}$$

Illuminance E_s represented by the surface density of the luminous flux incident on surface dA is defined by

$$E_s = \frac{dW}{dA}. \tag{5}$$

If area dA is illuminated by a point source located at distance r with luminosity I, then it is possible to derive the formula

$$E_s = \frac{I}{|r|^2} \cos\left(\theta\right). \tag{6}$$

It follows from (6) that the value of the point source illuminance is inversely proportional to the square of the distance between the source and the surface and is proportional to the cosine of the angle of incidence of the optic rays θ (Lambert cosine law), Fig. 2.

The listed basic quantities utilized to define the wide-spectrum electromagnetic wave can be determined by solving problems defined using PDEs, starting from static solutions, and passing through quasi-static to non-stationary solutions.

It has recently been demonstrated, in conjunction with the evolution of applications in areas above 100 THz, that the models of quantum physics based on the solution of Schrödinger's equation and the diffusion equation do not meet the requirements of preciseness and do not fit experiments in the wider spectrum of particular scientific areas. The models of its simplified formulations are transformed to formulations of the telegraphic equations or the wave equation. The field that treats the solution of models in nanoscale dimensions described by the telegraphic equation is discussed in [7–18].

If we now turn our attention back to the ultra wide band signal model, the UWB electromagnetic wave can, according to the principle of quantum mechanics, be described as noise.

3. THEORY OF LIGHTING, FROM THE ELECTROMAGNETIC POINT OF VIEW

In the theory of lighting the intensity and energy units are referred to in Watts and Joules. To convert noise temperatures into Kelvin units, we can use the Nyquist theorem for the noise power of a heated resistor $P_N = k\,T\,df$, where P_N [W] is the noise power, and $k = 1.38 \cdot 10^{-23}$ J/K is the Boltzmann constant, and df [Hz] is the spectrum bandwidth. As an illustration, we can estimate the noise power generated by the earlier noise source with excess noise ratio ENR ~ 30 dB, over 1 GHz bandwidth as 4 nW.

As in optics, we can calculate the energy of radiation as $e = hc/\lambda$, where e [J] is photon energy, $h = 6.63 \cdot 10^{-34}$ J/s is the Planck constant, and $c = 3.10^8$ m/s is the speed of light. Taking the wavelength of a typical microwave 0.1 m, with the other constants, we can see how weak the microwave photons are: $e = 20 \cdot 10^{-26}$ J.

A pair of electromagnetic waves or signals can interfere if both the elements have components of equal frequency. This is quantified by coherence, or more precisely by the (auto) correlation function R [19]. Two types of coherence are involved [20].

Temporal coherence generates an interference pattern in a device called an interferometer. In the Michelson interferometer, one wave is split in two; one part of it is delayed and then returned to a detector by reflectors. By varying the delay between the two wave trains, the detector output may vary as a function of the delay. We can detect interference by two independent wave trains if they have spectral components with an equal frequency and a steady phase. To achieve the best visibility of the fringes, the time delay should be adjusted to be $dt \approx 2\,\pi/d\omega = 1/df$, where dt is the coherence time. Therefore,

there is a quantity named the coherence length, or radius,

$$dL = \frac{2\pi c}{d\omega} = \frac{c}{df}. \tag{7}$$

For thermal light from a bulb, $df \sim 10^8$ Hz, $dt \sim 10^{-8}$ s, dL ~ 19 m. Laser light has a narrow bandwidth, $df \sim 10^4$ Hz or less than $dt \sim 10^{-4}$ s, and $dL \sim 190$ km. CW signals have $dL >$ a million kilometers.

To arrange interference, we can use (in addition to Michelson interferometers) "Lloyd's mirror". This structure is a simple flat or corner reflector by which a part of a wave beam is directed to the detector while the original wave enters the detector directly. Lloyd's mirror is often L-shaped for the best results, thus directing the beam by two consecutive reflections. It has been shown that the interference of different degrees of visibility can be observed for different noise bandwidth, or degree of coherence [21].

Spatial coherence is defined on a plane perpendicular to the direction of propagation. The coherence area is

$$A_c = \frac{r^2\lambda^2}{A_s}, \tag{8}$$

where r is the distance between the light source and a two-slot screen (as in Young's experiment) to generate fringes, A_s is the area of an (extended) source. The coherence volume is then the product of coherence length and coherence area

$$V_c = dL\,A_c \tag{9}$$

The light generated by heat as in an electric bulb or in glowing matter has almost no coherence (though Mandel and Wolf have found some [22]), in the same way as microwave noise sources. However, signals and waves carrying information in a narrow band, for example communication signals, radar waves and laser light, are highly coherent.

In optics, coherence length or coherence radius has been defined from the correlation function as the distance from a source where the autocorrelation function drops significantly [23]. For microwave noise, this definition had to be better established.

Using a wideband noise radiator and a radiometer, it was possible to define the "significant drop" of the correlation function to be one-half, or, as recognized by engineers, 3 dB. A wideband noise radiator typically generates a roughly rectangular spectrum. The corresponding correlation function has the form of $\sin(\tau)/\tau$. For zero delay, $R(0)$

corresponds to the noise-source power. The coherence radius measured for $R(\tau)$ decreasing from 1 to 0.5 dL can now be defined

$$dL = \frac{0.605\,c}{df},\qquad(10)$$

The use of the new definition of dL was tested with microwave radiometers at three frequencies and one microwave noise radiator. The noise bandwidth of this radiator was determined equally by both methods [24]. Fig. 5 shows the real experimental data taken with an 18-GHz radiometer, and Fig. 6 shows how the noise-radiator spectrum width was determined on the basis of only one measurement.
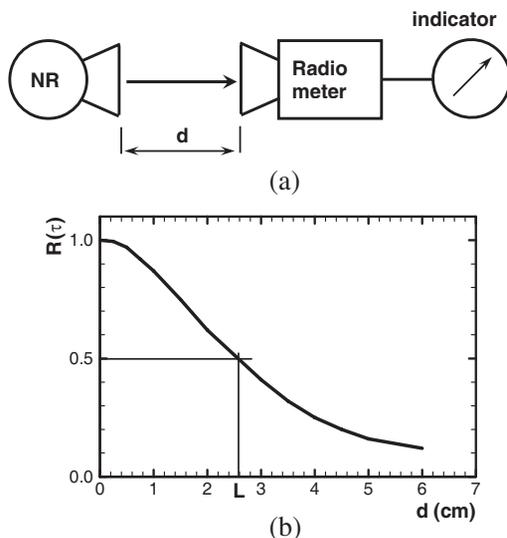

Figure 5. (a) Measuring coherence radius dL: set radiometer indication to 100% at any d, increase d till the indication decreases to 50%, the increment d is equal to dL. The graph shows the measured $R(\tau)$ function (b).

In addition to the effects of colored light, see Chapter 2, theory of lighting deals mainly with light intensity, and little importance is given to light wavelength. This kind of theory therefore seems to be suitable for describing partially coherent or incoherent radiation, e.g., microwave noise, which has a relatively wide bandwidth df around a center frequency, f. Let us study this approach further.
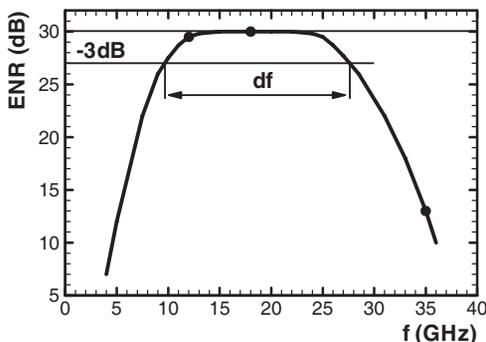
Figure 6. Noise radiator spectrum width measured: by three radiometers, at 12, 18 and 35 GHz (dots), by measuring dL at 18 GHz.

4. INTENSITY OF RADIATION

Using (2), we can define the spectral flux density of white light $\Phi_{e\lambda}$ [W] applied for the UWB signal generated by a microwave electromagnetic wave source. In opposite to the quantity $\Phi_{e\lambda}$, used in optics, microwave theory works with frequency f and not with a wavelength. Using the power flux density (brilliance) B [W/(m^{2}Hz sr)] defined by Planck's Radiation Law [3] and the basic relations in Chapter 2, we get the spectral flux density, which is an integral of B over a source surface

$$S = \iint_{\Theta} B \, d\Theta, \ \ [\text{W}/(\text{m}^2\text{Hz}), \ \text{or}, \ \text{Jansky}], \tag{11}$$

Spectral flux density S differs for different sections of the electromagnetic spectrum. For the microwave region, the Rayleigh-Jeans approximation is preferred, for $hf \ll kT$ in the form:

$$S = \frac{2 f^2 kT \, \Theta_s}{c^2} = \frac{2 \, kT \, \Theta_s}{\lambda^2}, \tag{12}$$

where Θ_s [sr] is the beam solid angle.

If an area A or its element, dA, is irradiated or radiates like in Fig. 4, the radiated power is described by Lambert's Law (6)

$$dW = B \cos(\theta) \, d\Theta \, dA \, df, \tag{13}$$

where B is the brilliance in the solid angle $d\Theta$ of the cone containing the radiation under angle θ from a normal to area element dA. Integrating over df and $d\Theta$ we will get the total ir/radiated power which, in white light theory, is the same as the power from (3).

One important contribution is often the "background ir/radiation", which can be obtained by integrating (13) over a hemisphere $\Theta = 2\pi$ (for terrestrial locations). For an incoherent background, the frequency distribution over the bandwidth can be assumed to be uniform; then, the full incident or emitted power to/from area A will be

$$W = A\,B\,df \iint\limits_{\Theta} \cos{(\theta)}\,d\Theta = \pi\,A\,B\,df. \qquad (14)$$

5. NOISE GENERATORS

In microwave technology, noise sources were developed for receiver testing. The earliest noise sources were gas-discharge tubes. Their main parameter was referred to as the "excess noise ratio" (ENR) [dB], and was defined as the ratio of the generated noise power to the noise power of a resistor matched to a particular transmission line, at ambient temperature. Gas-discharge tubes had a typical ENR of 15 dB, therefore 31.6 times the noise power generated by a matched resistor at an ambient temperature of $\sim 290\,\text{K}$.

The noise temperature was used as the technical measure of low noise levels. Therefore, an ENR of 15 dB means that a matched gas-discharge tube generated a noise temperature of $290 \times 31.6 = 9164\,\text{K}$. Gas-discharge noise tubes were used for more than 40 years thanks to their good stability over time, and the ambient temperature. Later, semiconductor pn diodes were used in the avalanche breakdown mode, and they gradually became a standard noise source, a source featuring overall stability and reliability. Their maximum ENR reaches $> 30\,\text{dB}$, so the generated noise temperature can be as high as 290 000 K.

For higher ENR, amplifiers can also be used at mm-wave frequencies, but the amplifier response affects the noise frequency spectrum. Amplifiers may be replaced by a spatial combination of multiple noise radiators [5].

6. NOISE RADIATORS AND ANTENNAS WITH RADIOMETERS

A radiometer with a suitable antenna is used to measure the intensity of the noise fields generated by noise radiators and attenuated, reflected or diffracted by various structures. This combination of a microwave radiometer with an antenna is sometimes called a microwave emission sensor [25], mainly because it can be used to detect object temperature over a distance. Another well-known and similar instrument is a radio telescope, which is sometimes capable of detecting the temperature of
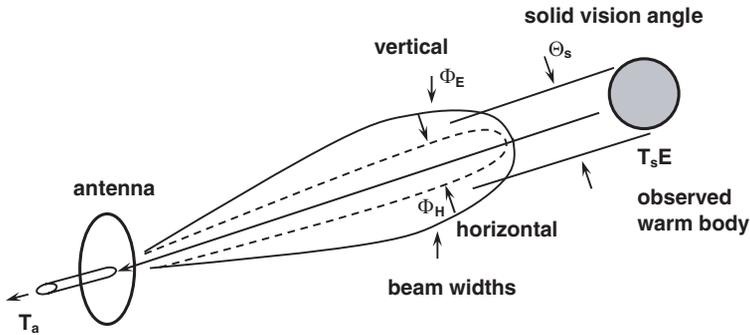
Figure 7. Radiometry principle: remote detection of the radiation of a distant body. An observed "warm" body with temperature T_s and surface emissivity E is seen from the antenna point within a solid "vision angle" Θ_s. The antenna radiation pattern has vertical beam width Θ_E, horizontal width Θ_H, and the beam solid angle is $\Theta_a = \Theta_E \cdot \Theta_H$.

a distant planet or galaxy. To explain how such remote sensors operate we refer to the principle of radiometry presented in Fig. 7.

Antennas are characterized by their radiation pattern (no gain is used here). A typical microwave antenna, e.g., a horn or a parabolic dish, has the main beam seen as a cone with a rounded end (other side lobes also exist but should be suppressed; in sensitive applications, their contribution must be accounted for).

As shown in Fig. 7, this directional antenna can be pointed at a distant object with physical temperature T_s, having emissivity E that usually depends on the frequency and observation angles. Emissivity has a value between 0 and 1, at $\Theta_a > \Theta_s$ we have $E = 1$. At the antenna output, a specific noise temperature T_a will appear

$$T_a = T_s E \frac{\Theta_s}{\Theta_a}, \tag{15}$$

where Θ_a is the solid angle of the antenna main beam, and Θ_s is the angle of vision of an observed target. The distance to an observed object is implied in the Θ_s/Θ_a ratio. If Θ_a is measured and known, it is possible to measure the temperature of a distant warm object quite reliably.

The above-mentioned principle of radiometry is also an illustration of geometrical optics applied to the microwave region. In fact, many microwave antennas are derived from optical telescopes. Parabolic reflectors are similar to the Newton telescope, while Cassegrainian and Gregorian optics are used in radio telescopes as well as in satellite communications and radar systems.

A directional antenna "looking" at a distant "large" object having temperature T_s (T can be affected by the object surface emissivity $E < 1$, $T = E \cdot T_s$) will receive the noise power [3], assuming in a resistor $W = kT$, and B or S defined by (12),

$$W = \frac{A_{ef}}{2} \iint B(\theta, \varphi) P_n((\theta, \varphi)) d\Theta = kT_a, \qquad (16)$$

where A_{ef} is the effective antenna aperture area, and $P_n(\theta, \phi)$ is the antenna radiation pattern depending on angles θ and φ (one main lobe assumed). Then for "singular" sources, we obtain

$$T_a = \frac{A_{ef}}{\lambda^2} \iint T_s(\theta, \varphi) P_n((\theta, \varphi)) d\Theta = \frac{1}{\Theta_a} \iint T_s P_n d\Theta. \qquad (17)$$

For "small" sources $\Theta_s \ll \Theta_a$ we finally get (15), assuming emissivity $E = 1$. This is often called the "radiometry equation", as it explains how the source temperature is translated into the antenna output temperature. The distance between a distant source and the antenna is "hidden" in the vision angle, Θ_s. In radio astronomy, and also in remote sensing, knowledge of the solid angle of a source and the calibrated antenna pattern enables us to make precise measurements of the temperatures of distant sources, see also Fig. 7.

7. NOISE PROPAGATION, DISPERSION, AND ATTENUATION

A noise-like wavefront is reflected by conductive objects as a coherent wave. For boundary refraction, Snell's law can be used. The dispersion in a lossy medium deserves a more detailed analysis [26]. We know from Equation (15) that the noise power is proportional to the antenna output temperature. As flux S passes through a lossy layer, it will change (decrease) in proportion to the layer attenuation α and absorbing length (depth) $\delta = 1/\alpha$:

$$S = S_1 e^{-\tau}. \qquad (18)$$

Quantity $\alpha x = \tau$ is often termed the "optical thickness" or "optical depth". Therefore, for $\delta = 1/\alpha$, $S = S_1/e = 0.368 S_1$. The same lossy layer, however, has its temperature T_o, and it therefore also emits its own noise radiation. The complete effect of the lossy layer on the passing radiation is

$$T'_s = T_s e^{-\tau} + T_o \left(1 - e^{-\tau}\right), \qquad (19)$$

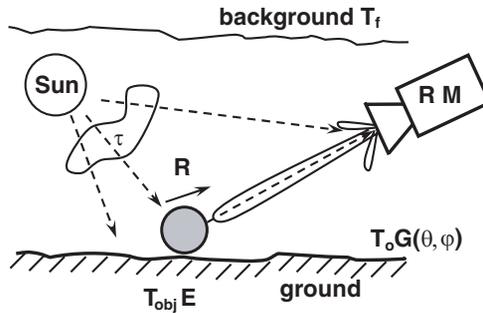where T_s is the source temperature, and $T_s \approx T_x E$, T_o is the lossy layer temperature.

Figure 8. Scene illumination and observation in remote sensing.

8. SCENE ILLUMINATION AND OBSERVATION

Figure 8 presents an example of a remote-sensing scene being observed by an antenna with a radiometer [26]. We can see a striking similarity with the use of a light-intensity meter placed in the hand of a person evaluating the lighting of a similar scene. The radiometer sensor receives the following noise temperature contributions: object emission, $T_{obj}E$, earth emission, $T_oG(\theta, \varphi)$, often including a contribution from side lobes, background plus medium (air) emission, T_f (may include precipitations), and solar radiation reflected from the object (sometimes also from Earth), $T_sR\Theta_s/\Theta_a$. The total received temperature at the antenna output will be

$$T_a = T_{obj}E(f) + T_oG(\theta, \varphi) + T_f\left(1 - e^{-\tau}\right) + T_sR\frac{\Theta_s}{\Theta_a}. \qquad (20)$$

In remote sensing observations, wanted (and unwanted) objects have specific "signatures". For example: frequency (wavelength) variations, vision angle (compensated by antenna scanning), emissivity (frequency and angle-dependent). To find an optimum solution, multi-spectral sensors, complex antennas, scanning and truth tests are used.

9. SIMILARITIES BETWEEN LIGHTING AND MICROWAVE NOISE FIELDS, EXPERIMENTS

Returning to the problem of lighting, we can state that the human eye perceives wideband "white" light more pleasantly than the monochromatic light of a laser or a discharge tube. Microwave noise seemed to have no other importance than its suitability for testing sensitive receivers. Its incoherence, however, has provided interesting

applications in sensors and antenna studies. Noise waves do not interfere, therefore the tested objects can move; further, it is possible to probe the field intensity close to or even inside antennas and radiators. The absence of interference has enabled very sensitive measurement of the field distribution of surface leaky waves excited in planar transmission lines [27]. If a monochromatic wave is used, the field distribution of leaky waves is significantly masked by reflections at the substrate edges.

Interesting experiments have been carried out to repeat the well-known optical experiments in the microwave region. For example, Young's two-slit experiment was run with microwave noise [28], and no fringes were detected, Fig. 9. Radiometric measurement here shows only simple superposition of fields coming from the two noise sources. Similarly, a Lloyd's mirror test did not reveal any interference effects with microwave noise. On the other hand, the Fabry-Perot interferometer experiment with high-permittivity dielectric plates used as parallel boundaries in the resonator showed varying degree of coherence for different noise bandwidths [21].
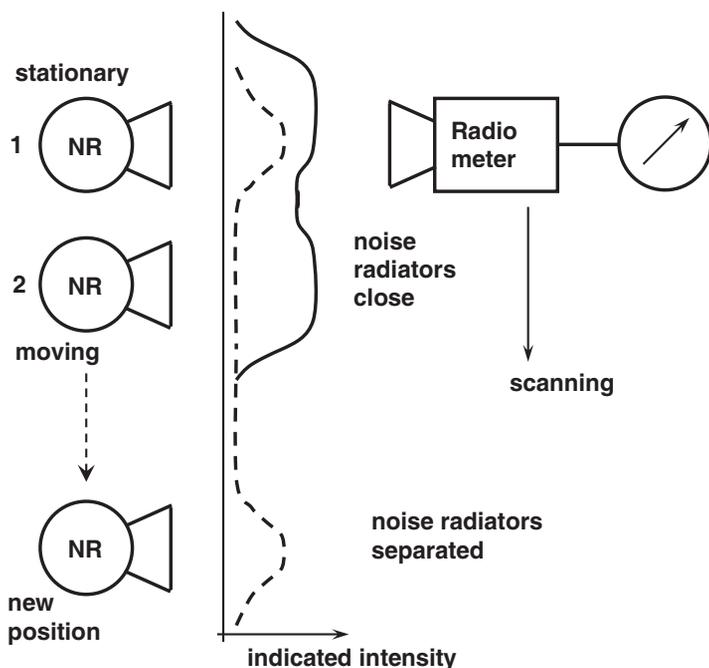
Figure 9. Young's experiment with two microwave noise radiators. Radiometer output plot, intensity versus distance is smooth, no fringes.
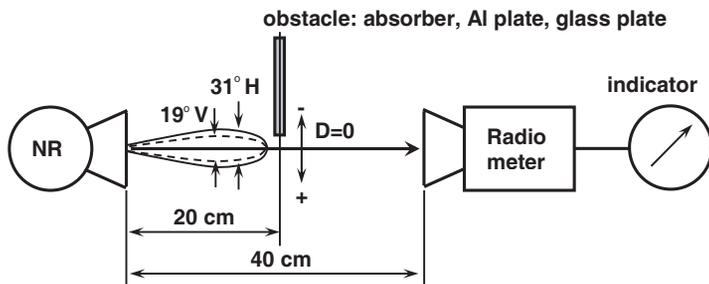
Figure 10. Noise-field shadowing experiment: obstacle gradually covering the beam of a noise radiator: beam widths shown for vertical and horizontal setting.
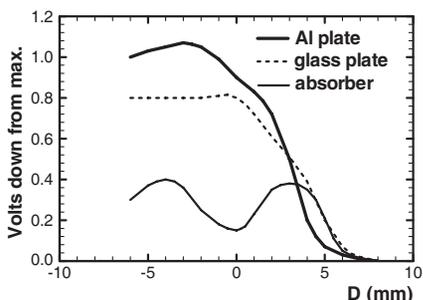

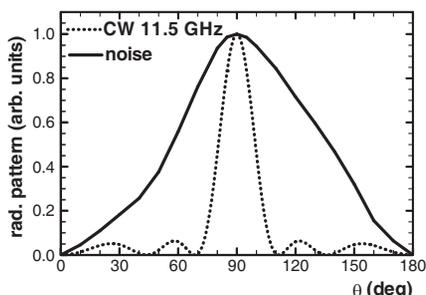**Figure 11.** Shadowing test results, vertical polarization along obstacle edge.

Figure 12. Radiation patterns of the two matrices of 3×3 radiators.

Recently, a "shadowing experiment" was performed with a microwave noise radiator as the "light" source and a radiometer as the detector. Between these two, a shadowing wall was moved across the axis, as shown in Fig. 10. The results are shown in Fig. 11 for the (linear) polarization set parallel to the edge of the obstacle wall. Normal polarization shows similar behavior. The wall material was aluminum, glass, and a microwave absorber. The results show that the noise wave behaves in exactly the same way as light.

A 3×3 matrix of microwave noise radiators was tested to prove that the radiated noise power can be augmented without amplifiers [5]. The noise generator central frequency is 11.5 GHz, and the bandwidth is about 1.5 GHz. The measured radiation pattern is plotted in Fig. 12. No interference was observed, and no coupling similar to antenna arrays using coherent signals was found either. The noise power density on the antenna axis was "amplified" more than 5 times. Fig. 12 shows

the simulated radiation pattern of the 3×3 matrix of $\lambda/2$ dipoles located at the same positions as the noise radiators [5]. The dipoles are fed in phase with equal amplitudes by a monochromatic signal at 11.5 GHz. The influence of interferences is clearly visible, and contrasts with the simple superposition of noise fields.

In technical applications, we often encounter conjugated problems. Modeling and experimental verification of results is a necessary part of the design process during the development and measurement of light sources. This problem was solved by transforming optical quantities into thermal field quantities represented by a noise field in the THz area. The formulation of the basic thermal model is based on the first law of thermodynamics. The problem was finally solved by the ANSYS program, using the finite elements method [2, 29]. Fig. 13 shows the distribution of the light intensity produced by a standard electric 240 V filament lamp located in a shield on a screen placed 40 cm below it. A relatively good fit between the calculated and experimental data can be observed.
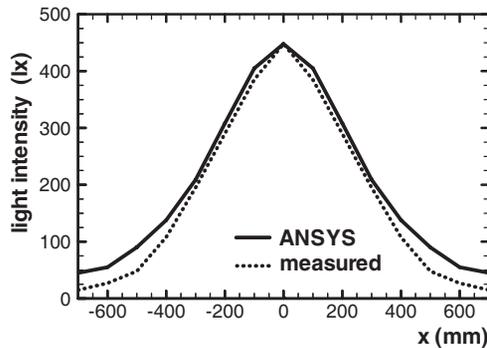

Figure 13. Distribution of the light intensity radiated by a filament lamp.

The concept of lighting also relates particularly to imaging and/or photographing various objects, while the natural or artificial light sources are arranged in such a way that the object image is well distinguished against the background. In this paper, we do not study these phenomena; for example, image "sharpness" and contrast have been studied in books on Radio Astronomy in the form of describing various antennas as "spatial filters" with adjusted beam width, in the form of scanning a scene, etc.

Recently, Optical Coherence Tomography (OCT) has become a useful diagnostic tool in ophthalmology. The light source is intentionally incoherent, and the interferometer response is therefore
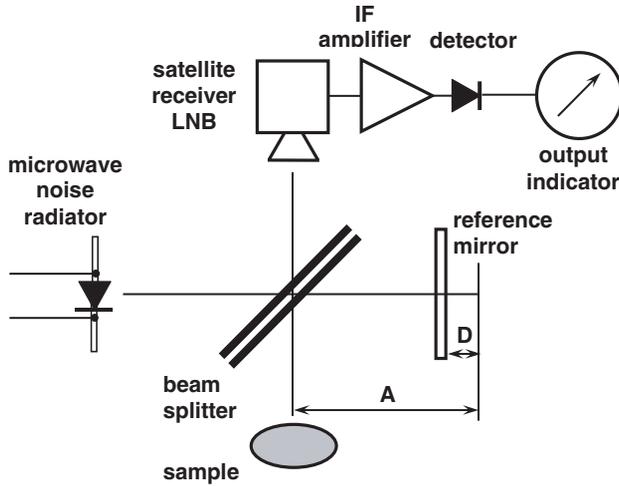
Figure 14. Microwave coherence tomography setup with the Michelson interferometer [30]. The reference mirror was moved to "scan" the depth profile of the tested samples, 5 cm approx. Radiometer with center frequency $\sim 11\,\text{GHz}$, and noise bandwidth $\sim 1\,\text{GHz}$, and the noise radiator used in [25] are applied.

not determined by the probing wavelength, but by a wave packet generated by the target structure. Polivka successfully tested OCT principles in his experiments with Microwave Coherence Tomography, as shown in Fig. 14 [30].

10. CONCLUSION

In the study presented here, we have attempted to establish a certain background of a microwave noise field behaving similarly to white light. Wherever the frequency or wavelength is used in the equations, it is understood that it is a center frequency or wavelength of a wideband noise spectrum. Coherence features were used in theory and experiments to demonstrate the low level of interference, mostly in the near field zone close to noise radiators. A new definition of coherence length was introduced for the purpose of establishing the noise field bandwidth by a single measurement. The microwave noise field was shown to behave similarly to white light.

The paper compared the behavior of the noise field with white light ($\lambda \in <\,400\,\text{nm},\ 700\,\text{nm}>$), and showed ways of quantitative description of optical signals and models subsequently applied in the

area of UWB signals. The description of the microwave noise fields has been supported by a number of experiments showing the usefulness of noise field applications. The most important feature of non-coherent noise fields is the absence of interference effects that in many cases mask the investigated behavior of the wave.

Classical optics has evolved according to Helmholtz monochromatic theory. Monochromatic fields stimulate various interference effects. The approach presented in this text is quite opposite and fully innovative. The investigation of microwave noise fields has clarified the nature of wide band noise optics, which is treated only marginally in the theory of lighting. The main contribution of this paper lies in establishing the fundamentals of a unified theory of lighting using white light with experiments in the area of noise fields.

ACKNOWLEDGMENT

REFERENCES

1. Van Vlaenderen, K. J., "A charged space as the origin of sources, fields and potentials," http://xxx.lanl.gov/, arXiv:physics/9910022 v1, October 16, 1999.

2. Kadlecova, E., "Automated system of calculation of reflecting surface of light sources," Ph.D. thesis VUT in Brno, FEKT, Brno, September 2004.

3. Kraus, J. D., *Radio Astronomy*, McGraw-Hill, New York, 1967.

4. Polivka, J., "Microwave noise radiators," *International Journal of Infrared and Millimeter Waves,* Vol. 17, No. 10, 1779–1788, October 1996.

5. Polivka, J., "Spatial combination of multiple microwave noise radiators," *High Frequency Electronics*, 46–53, April 2008.

6. Habel, J., et al., *Lighting Technic and Illumination*, 448 pages, FCC Public, Prague, 1995.

7. Costa-Quintana, J. and F. Lopez-Aguilar, "Propagation of electromagnetic waves in material media with magnetic monopoles," *Progress In Electromagnetics Research*, Vol. 110, 267–295, 2010.

8. Chang, H.-W. and S.-Y. Mu, "Semi-analytical solutions of 2-D homogeneous helmholtz equation by the method of connected local

fields, *Progress In Electromagnetics Research*, Vol. 109, 399–424, 2010.

9. Lim, J., J. Lee, J. Lee, S. Han, D. Ahn, and Y. Jeong, "A new calculation method for the characteristic impedance of transmission lines with modified ground structures or perturbation," *Progress In Electromagnetics Research*, Vol. 106, 147–162, 2010.

10. Hofer, W. A., "A dynamic model of atoms: Structure, internal interactions and photon emissions of hydrogen," http arXiv:quant-ph/9801044v2, June 8, 2000.

11. Popov, E., N. Bonod, and M. Neviere, "Light transmission through a single subwavelength aperture aperture in a lossy screen," *PIERS Proceedings*, 1451–1455, Beijing, China, March 26–30, 2007.

12. Cui, J.-P. and W.-Y. Yin, "Transfer function and compact distributed RLC models of carbon nanotube bundle interconnets and their applications," *Progress In Electromagnetics Research*, Vol. 104, 69–83, 2010.

13. Topa, A. L., C. R. Paiva, and A. M. Barbosa, "Electromagnetic wave propagation in chiral H-guides," *Progress In Electromagnetics Research*, Vol. 103, 285–303, 2010.

14. Dong, J., "Exotic characteristics of power propagation in the chiral nihility fiber," *Progress In Electromagnetics Research*, Vol. 99, 163–178, 2009.

15. Kimble, H. J., "The quantum internet," *Nature*, Vol. 453, 1023–1042, Insight review, June 19, 2008.

16. Lee, H.-S., "A photon modeling method for the characterization of indoor optical wireless communication, *Progress In Electromagnetics Research*, Vol. 92, 121–136, 2009.

17. Anantram, B., et al., "Modeling of nanoscale devices," *Proceedings of the IEEE*, Vol. 96, No. 9, 1511–1550, September 2008.

18. Yu, G. X., T. J. Cui, W. X. Jiang, X. M. Yang, Q. Cheng, and Y. Hao, "Transformation of different kinds of electromagnetic waves using metamaterials," *Journal of Electromagnetic Waves and Applications*, Vol. 23, 583–592, 2009.

19. Dunn, P. F., *Measurement and Data Analysis for Engineering and Science*, McGraw-Hill, New York, 2005.

20. Wolf, E., *Theory of Coherence and Polarization of Light*, Sections 3 and 5, Cambridge Univ. Press, New York, 2007.

21. Kapilevich, B. and J. Polivka, "Noise versus coherency in mm-wave material characterization," *IR MM-THz Wave Conference*,

15–19, CalTech, Pasadena, California, September 2008.

22. Mandel, L. and E. Wolf, "Coherence of thermal radiation," *Uspekhi Fizicheskich Nauk*, Part 1, t. 87, 492, 1965; Part 2, t. 88, 347, 1966; Part 3, t. 88, 619, 1966 (in Russian).

23. Born, M. and E. Wolf, *Principles of Optics*, Pergamon Press, 1980.

24. Polivka, J., "Active microwave radiometry," *International Journal of Infrared and Millimeter Waves*, Vol. 16, No. 3, 483–500, March 1995.

25. Polivka, J., "Overview of microwave sensor technology," *High Frequency Electronics*, 32–42, April 2007.

26. Polivka, J., "Microwave radiometry and applications," *International Journal of Infrared and Millimeter Waves*, Vol. 16, No. 9, 1593–1672, September 1995.

27. Zehentner, J., J. Macháč, J. Mrkvica, M. Sarnowski, and J. Polívka, "Field mapping by active radiometry," *Proceedings of the 1998 Asia-Pacific Microwave Conference*, Vol. 1, 217–220, Yokohama, Japan, December 1998.

28. Polivka, J., "Noise can be good, too," *Microwave Journal*, Vol. 47, 66–78, March 2004.

29. Kadlecova, E. and P. Fiala, "Numerical modelling of the special light source with novel R-FEM method," *PIERS Online*, Vol. 2, No. 6, 644–647, 2006.

30. Polivka, J., "Experiments with microwave coherence tomography," Part 1, *High Frequency Electronics*, Vol. 5, 36–40, July 2006. Part 2, *High Frequency Electronics*, Vol. 5, 36–43, August 2006.